Optimization Strategies for Simulated Moving Bed and PowerFeed Processes

Yoshiaki Kawajiri and Lorenz T. Biegler
Dept. of Chemical Engineering, Carnegie Mellon University, Pittsburgh, PA, 15213

DOI 10.1002/aic.10736
Published online December 8, 2005 in Wiley InterScience (www.interscience.wiley.com).

Simulated moving bed (SMB) processes have been applied to many important separations in sugar, petrochemical, and pharmaceutical industries. However, systematic optimization of SMB is still a challenging problem. Two tailored approaches are proposed, full discretization and single discretization, where both the optimal operating condition and concentration profiles are obtained by a Newton-type solver. In a case study of fructose and glucose separation, it has been found that the full-discretization method implemented on AMPL with IPOPT is more efficient than single-discretization method on gPROMS with SRQPD. The reliability of the full-discretization method is also demonstrated with case studies of a bi-Langmuir isotherm and a PowerFeed optimization problem. © 2005 American Institute of Chemical Engineers *AIChE J,* 52: 1343-1350, 2006
Keywords: simulated moving bed, chromatography, powerfeed, dynamic optimization, interior-point method

Introduction

Simulated moving bed (SMB) chromatography has been gaining more attention since its emergence in the 1960's. Its application areas include sugar, petrochemical, and pharmaceutical separations. In particular, enantiomeric separations have been found to be one of the most effective applications in the past decade.

An SMB system consists of multiple columns connected to each other making a circulation loop (Figure 1). Between every column, there are inlet ports for feed and desorbent streams, as well as outlet ports for extract and raffinate streams. The feed and desorbent are supplied continuously and at the same time extract and raffinate are drawn continuously through the ports. These four inlet/outlet ports are switched simultaneously at a regular interval in the direction of the liquid flow. This system does not reach a steady state, but a cyclic steady state (CSS), where the concentration profiles change dynamically, and the profiles of both liquid and solid phase at the beginning of a cycle are identical to those at the end of the cycle.

Correspondence concerning this article should be addressed L. T. Biegler at lb01+@andrew.cmu.edu.

Determining the design and operating parameters of SMB processes remains a challenging problem. The cyclic dynamics characterized by CSS complicate numerical treatments. In most circumstances of industrial SMB process development, the design and operating parameters are determined by trial-and-error approaches, where dynamic simulations are repeated, and the operating parameters are changed manually after every simulation run. In order to avoid this time-consuming process, several approaches are developed that systematically optimize SMB operations. Stochastic optimization approaches, as well as Newton-based approaches have been proposed (for example, Subramani et al.[1] Dünnebier and Klatt[2]). Currently, development of efficient optimization methods of SMB processes is an active research area.

Many new kinds of SMB operations have been proposed to enhance productivity. Traditional SMB systems keep the liquid velocities constant during a step, and then switch the four inlet/outlet streams at the same time. In PowerFeed systems, however, the velocities become time-variant. Moreover, VARICOL systems perform asynchronous valve switching, where the four inlet/outlet ports are switched independently, not simultaneously.[3-5] Since the degrees of freedom become significantly larger in these systems, the importance of an efficient and systematic optimization strategy becomes more significant.

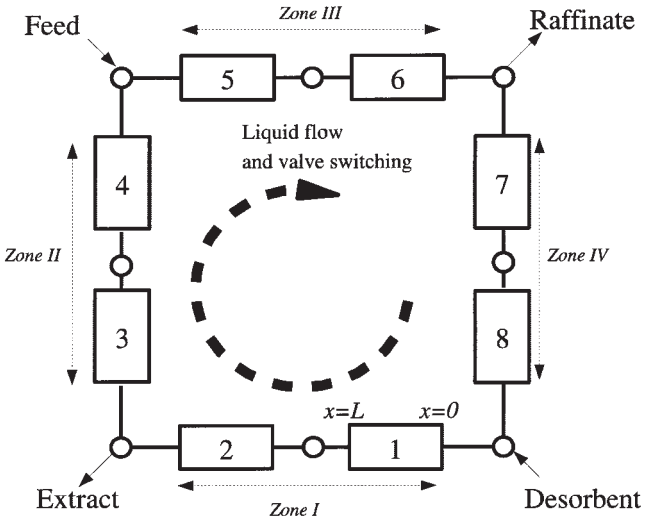

Figure 1. SMB: 8 column type with two columns in each zone

In this study, we develop two optimization strategies for SMB processes that rely on spatial and temporal discretizations. The first requires only a spatial discretization and applies a sequential dynamic optimization algorithm, while the second requires a temporal and spatial discretization and applies a fully simultaneous optimization approach. In particular, we show that the simultaneous approach is very efficient and well suited for SMB optimization. We begin by describing the SMB model followed by the objective function and CSS constraints. We then describe both optimization strategies. These strategies are compared on the first case study with a linear isotherm, where the advantages of the simultaneous approach are observed. In the second case study, a more challenging system is considered with a nonlinear isotherm. Moreover, in both case studies we show that the simultaneous approach is well-suited for SMB optimization with dynamic feeding strategies.

Mathematical Modeling of SMB

In order to reduce the effort for model identification as well as numerical difficulties, it is crucial to choose a simple mathematical model without losing accuracy. In this work, it is assumed that there is no radial distribution in the columns, and the thermal and pressure effects are negligible.

Band broadening in a chromatographic column is caused by axial dispersion, mass transfer resistance, and dispersion into the adsorbent particles. Of there three effects, axial dispersion and mass-transfer resistance are often lumped together into either effect. Reports which discuss the validity of this assumption can be found elsewhere.[2,6,7] For the diffusion into the particles, linear driving force (LDF) models have been successfully applied to SMB processes regardless of the choice of linear or Langmuir isotherms.[8,9] From these considerations, we employ the following model equations:

Mass balance in the liquid

$$\varepsilon_b \frac{\partial C_{n,i}(x,\,t)}{\partial t} + (1-\varepsilon_b)\frac{\partial q_{n,i}(x,\,t)}{\partial t} + u_m(t)\frac{\partial C_{n,i}(x,\,t)}{\partial x} = 0 \tag{1}$$

Mass balance in the adsorbent:

Liquid phase based

$$(1-\varepsilon_b)\frac{\partial q_{n,i}(x,\,t)}{\partial t} = K_{appl,i}(C_{n,i}(x,\,t) - C^{eq}_{n,i}(x,\,t)) \tag{2}$$

or *Solid phase based*

$$\frac{\partial q_{n,i}(x,\,t)}{\partial t} = K_{apps,i}(q^{eq}_{n,i}(x,\,t) - q_{n,i}(x,\,t)) \tag{3}$$

Isotherm:

Liquid phase based

$$q_{n,i}(x,\,t) = f(C^{eq}_{n,i}(x,\,t)) \tag{4}$$

or *Solid phase based*

$$q^{eq}_{n,i}(x,\,t) = f(C_{n,i}(x,\,t)) \tag{5}$$

Boundary condition

$$C_{n,i}(0,\,t) = C^{in}_{n,i}(t), \qquad i = 1,\ldots,N_c,$$
$$n = 1,\ldots,N_{Column}, \quad m = I,\,II,\,III,\,IV \tag{6}$$

where ε_b is the void fraction, $C_{n,i}$ (x,t) is the concentration in the liquid phase of component i in column n, $q_{n,i}$ (x,t) is the concentration in the solid phase, $C^{in}_{n,i}(t)$ is the inlet concentration to n th column, u_m (t) is the superficial liquid velocity in zone m, $C^{eq}_{n,i}(x,\,t)$ is the equilibrium concentration in the liquid phase, $q^{eq}_{n,i}(x,\,t)$ is the equilibrium concentration in the solid phase, $K_{apps,i}$ and $K_{appl,i}$ are the solid-phase based and liquid-phase based mass-transfer coefficient, respectively. The subscripts i correspond to chemical components, n the index of columns, and m the zone number *I, II, III,* and *IV*, as shown in Figure 1. N_c is the total number of components, N_{column} is the number of columns, and N is the number of columns in zone m, with $N_I + N_{Ii} + N_{III} + N_{IV} = N_{Column}$.

Referring to Figure 1, the mass balances at each inlet/outlet port are given by:

Desorbent inlet port

$$u_{IV}(t) + u_D(t) = u_I(t) \tag{7}$$

$$C^{in}_{1,i}(t)u_I(t) = C_{N_{Column},i}(L,\,t)u_{IV}(t) \tag{8}$$

Extract outlet port

$$u_I(t) - u_E(t) = u_{II}(t) \tag{9}$$

$$C^{in}_{N_I+1,i}(t) = C_{N_I,i}(L,\,t) \tag{10}$$

Table 1. Parameters of Fructose/Glucose Separation

Parameter	Value	Parameter	Value
ε_b	0.389		
K_1	0.518	$K_{apps\,1}$ [1/s]	6.84×10^{-3}
K_2	0.743	$K_{apps\,2}$ [1/s]	6.84×10^{-3}
$C_{F,1}$ [%]	50	$C_{F,2}$ [%]	50

Feed inlet port

$$u_{II}(t) + u_F(t) = u_{III}(t) \tag{11}$$

$$C_{N_I+N_{II},i}(L, t)u_{II}(t) + C_{F,i}(t)u_F(t) = C^{in}_{N_I+N_{II}+1,i}(t)u_{III}(t) \tag{12}$$

Raffinate outlet port

$$u_{III}(t) - u_R(t) = u_{IV}(t) \tag{13}$$

$$C^{in}_{N_I+N_{II}+N_{III}+1,i}(t) = C_{N_I+N_{II}+N_{III},i}(L, t) \tag{14}$$

where $u_D(t)$, $u_E(t)$, $u_F(t)$, $u_R(t)$ are the superficial velocities (flow rates divided by cross-sectional area of column) of the desorbent, extract, feed, and raffinate, respectively. At the CSS, the concentration profiles are identical at the beginning and at the end of a cycle. Since SMB repeats the same operation for the number of columns, the profiles at the beginning of a step are identical to those of the downstream adjacent column at the end of the step

$$C_{n,i}(x, 0) = C_{n+1,i}(x, t_{step}), \qquad n = 1, \ldots, N_{Column} - 1 \tag{15}$$

$$q_{n,i}(x, 0) = q_{n+1,i}(x, t_{step}), \qquad n = 1, \ldots, N_{Column} - 1 \tag{16}$$

$$C_{N_{Column},i}(x, 0) = C_{1,i}(x, t_{step}) \tag{17}$$

$$q_{N_{Column},i}(x, 0) = q_{1,i}(x, t_{step}) \tag{18}$$

Optimization Strategy and Treatment of CSS Condition

We consider a throughput maximization problem of SMB processes with purity and recovery requirements of the extract product. It can be formulated as a dynamic optimization problem that maximizes the average feed velocity $\bar{u}_F$:

$$\max_{u_I(t),u_{II}(t),u_{III}(t),u_{IV}(t),t_{step}} \bar{u}_F := \frac{1}{t_{step}} \int_0^{t_{step}} u_F(t)dt \tag{19}$$

subject to

$$(\text{Extract Product Purity}) = \frac{\int_0^{t_{step}} u_E(t)C_{E,k}(t)dt}{\sum_{i=1}^{N_C} \int_0^{t_{step}} u_E(t)C_{E,i}(t)dt} \geq Pur_{\min} \tag{20}$$

$$(\text{Extract Product Recovery}) = \frac{\int_0^{t_{step}} u_E(t)C_{E,k}(t)dt}{\int_0^{t_{step}} u_F(t)C_{F,k}(t)dt} \geq \text{Rec}_{\min} \tag{21}$$

$$u_l \leq u_m(t) \leq u_u \tag{22}$$

where $C_{E,i}(t)$ is the concentration of the component i in the extract stream

$$C_{E,i}(t) = C_{N_I,i}(L, t) \tag{23}$$

t_{step} is the valve switching interval, or step time, $Pur_{\min}$ and $Rec_{\min}$ are the purity and recovery requirements of the desired product which should be recovered in the extract stream, respectively. The desired product is denoted by the index k. u_u and u_l are the upper and lower bounds on the zone velocities, respectively. The variables are constrained by the mass balance Eqs. 1–14 and CSS condition (Eq. 15–18).

Nested, single-discretization approach

This straightforward optimization approach is to mimic the actual start-up process, by solving the partial differential equation (PDE) model for a large number of cycles until the SMB reaches the CSS, and then the entire calculation is repeated until the optimal operating parameters are found. Since the model is integrated in time for a large number of cycles, the efficacy of this approach heavily depends on the performance of the integrator. In the approach proposed by Toumi et al.[5] and Dünnebier and Klatt[2], the PDEs are discretized in space, and turned into a mixed set of differential algebraic equations (DAEs). The resulting DAEs are integrated repeatedly until the differences of concentration profiles at the beginning of a cycle and at the end become less than a constant tolerance; then the objective function and constraints are evaluated. The derivatives of the state variables with respect to the decision variables are obtained by finite difference.

Method (A): simultaneous, single-discretization approach

In order to reduce the computational effort associated with the temporal integration, Jiang et al.[10] proposed a simultaneous approach for PSA processes. In this approach, a Newton solver searches for both the optimal operating parameters and concentration profiles simultaneously. The discretized concentration nodes at the beginning of a cycle are treated as part of the decision variables. Since the number of variables that Newton solver handles increases, the performance of the solver becomes more crucial. For the computation of the first derivatives

Table 2. Initial Operating Conditions

Variable	Initial Value
$\bar{u}_I$ [m/h]	8.0
$\bar{u}_{II}$ [m/h]	5.00
$\bar{u}_{III}$ [m/h]	5.01
$\bar{u}_{IV}$ [m/h]	3.50
$\bar{u}_F = \bar{u}_{III} - \bar{u}_{II}$ [m/h]	0.01
t_{step} [s]	1140

Table 3. Comparison of Optimal Solutions Obtained using Methods (A) and (B)

	Method (A) (gPROMS) $N_{FEX} = 40$	Method (B) (AMPL/IPOPT) $NFEX = 40$ $N_{FET} = 5$, $N_{COL} = 3$	Method (B) (AMPL/IPOPT) $NFEX = 40$ $N_{FET} = 20$, $N_{COL} = 3$
$\bar{u}_F$ [m/h] (obj. fcn. value)	0.5216	0.5210	0.5212
$\bar{u}_{II}$ [m/h]	3.7361	3.7391	3.7318
$\bar{u}_{III}$ [m/h]	4.2577	4.2601	4.2530
$\bar{u}_{IV}$ [m/h]	3.1259	3.1296	3.1223
t_{step} [s]	1415	1415	1417
Purity of fructose [%]	90.0	90.0	90.0
Recovery of fructose [%]	80.0	80.0	80.0
CPU time (min)	111.8	1.53	20.48
Number of iterations	38	39	59

with respect to the decision variables, sensitivity equations are integrated along with the DAEs. Toumi[4] applied this approach to SMB and PowerFeed processes. In his work, optimization performance of two different interpretations of CSS constraints is compared: one with the same CSS constraints as described in Eqs.15–18, and the other that is based on a single column model. Here, this model is executed step by step over the cycle, with temporal outlet profiles stored at a given step and retrieved as inlet profiles in the next step. CSS is achieved by enforcing constraints that match the spatial column profiles at the beginning and the end of the cycle. In this study, we apply the former approach and implement it on gPROMS.

Method (B): simultaneous, full-discretization approach

Nilchan[11] proposed a fully discretized approach for rapid pressure swing adsorption (RPSA) systems, where the model is discretized both in time and space, turning the PDE constrained optimization problem into a large-scale optimization problem constrained by algebraic equations. The computational effort for the model integration is eliminated at the expense of the higher number of variables. The drawback of this approach is that if the concentration profiles are steep, a finer finite element discretization is required, resulting in creating a huge number of variables. Ko et al.[12] reported that in their optimization scheme of PSA processes implemented on gPROMS, Method (B) is computationally more expensive than Method (A). Also, they obtained a different optimization result because of the less accurate discretization. Kloppenburg and Gilles[3] also applied this simultaneous approach to SMB systems using LANCELOT in AMPL. They reported that the solver performance was unsatisfactory, but concluded that finer parametrization of control variable will be possible *as better optimization methods become available.*

In this study, we reconsider this approach with a different discretization method and more recent optimizer. In particular, we apply Radau collocation on finite elements for temporal discretization.[13,14] Since the performance of this approach solely depends on the optimization solver, it is crucial to choose an efficient solver. In this study, we choose IPOPT, an interior point method solver that uses the exact second derivative information. IPOPT has superior convergence properties along with efficient handling of inequality constraints and sparse structure of the linearized KKT conditions.[15]

Case Study 1: Linear Isotherm

As the first case study, we consider a linear isotherm, as in Hashimoto et al.[9], for the separation of fructose and glucose

$$q_{n,i}(x, t) = K_i C^{eq}_{n,i}(x, t) \tag{24}$$

The mass balance equation based on the liquid phase Eq. 2 is used. The model parameters are shown in Table 1. We set the column length to $L = 2.0$ m, and the number of columns $N_{\text{Column}} = 4$, with one column in each zone, that is, $N_m = 1$, $m = I, II, III, IV$.

Constant zone velocities

Method (A). First we consider the optimization problem (Eq. 19 – 21) with constant zone velocities. The value of the fastest zone velocity $u_I(t)$, is fixed at its upper bound u_u. We implement the optimization problem using Method (A) on gPROMS with $Pur_{\text{Min}} = 90\%$, $Rec_{\text{Min}} = 80\%$, $u_l = 0.1$ m/h, and $u_u = 8.0$ m/h. The centered finite difference method is used for the spatial discretization. We set the number of finite elements for spatial discretization N_{FEX} to be 40 per column, which we confirm to be large enough by comparing several discretizations on a number of simulation runs. We also find an initial operating condition that satisfies all constraints by running a few trial and error simulations (Table 2). The operating condition and resulting concentration profiles are supplied to the NLP solver, SRQPD, as the starting point. The problem handled by SRQPD has 644 variables, 640 equality constraints, two inequality constraints, and three lower and upper bounds. The discretized PDEs, as well as the sensitivity equations are integrated from $t = 0$ to $t = t_{\text{step}}$ in each function evaluation. SRQPD finds the optimal solution in 111.8 min on a Pentium IV 2.8 GHz Linux machine. Here the optimal feed velocity is over 50 times the initial one. The optimal operating condition and concentration profiles are shown in Table 3 and Figure 3, respectively.

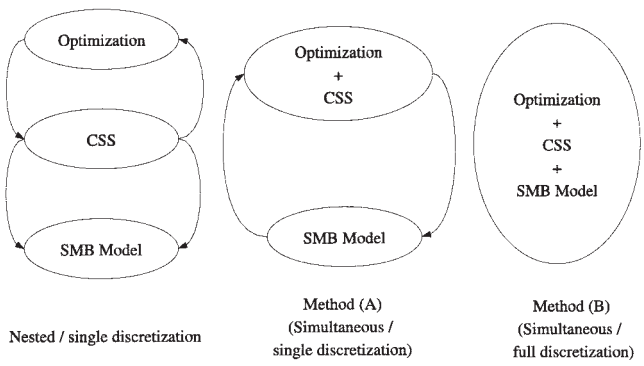

Figure 2. Optimization approaches.

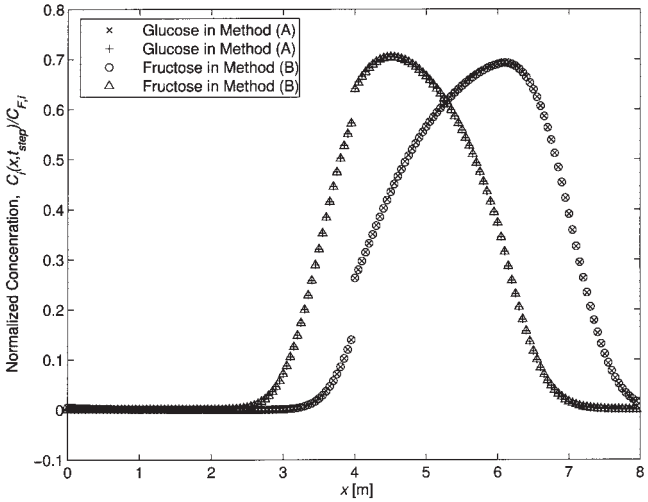

Figure 3. CSS profiles: Optimal solutions using Methods (A) and (B). N_{FEX} =40 for both methods and N_{FET}=5 for Method (B)

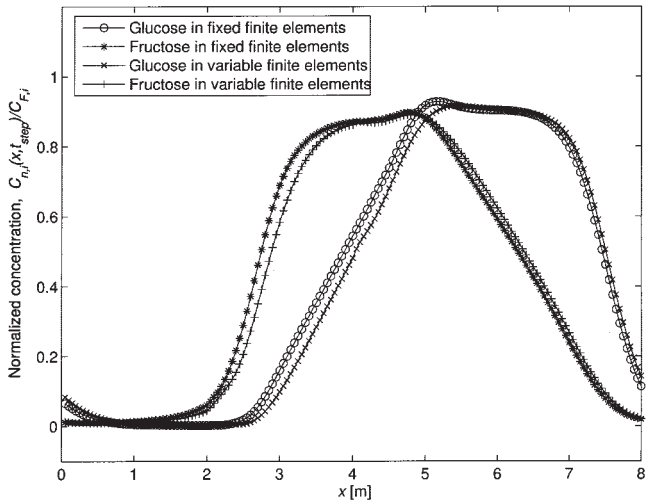

Figure 5. Optimal concentration profiles for fructose and glucose separation with N_{FET} = 5: Fixed finite elements of time and variable finite elements.

Method (B). We also implement the same optimization problem with Method (B) using IPOPT within the AMPL modeling environment. The spatial domain is discretized using the same method as Method (A), that is, N_{FEX} is set to 40. Several temporal discretizations were also considered (up to N_{FET} = 20) and N_{FET} = 5 was found to be accurate, as seen below. Hence, the number of finite elements for temporal discretization, N_{FET} is set to 5, and the number of collocation points in each finite element, N_{COL} is set to 3. Before solving the optimization problem, we get the initial concentration profiles by fixing all operating conditions $\bar{u}_{II}$, $\bar{u}_{III}$, $\bar{u}_{IV}$ and t_{step}, and solve the initialization problem using IPOPT. The solution is found in 2.9 CPU seconds. Then the initial concentration profiles and initial operating condition are given to the optimization problem. The number of variables in the resulting NLP is 33999, and number of equations is 33995. IPOPT finds the optimal solution in 1.53 CPU min on the same Pentium IV machine. As can be seen in Figure 3 and Table 3, the optimal solutions obtained by Method (A) and Method (B) are virtually identical. Here, even when N_{FET} is increased from 5 to 20, the variation of the optimal solution is within 0.1 %, and no change of the optimal concentration profiles can be seen. This confirms that the finite elements are suitable. Moreover, as seen in Table 3, IPOPT remains efficient and reliable even when the number of finite elements is increased. From these results, we conclude that Method (B) with our implementation scheme is more efficient in this case study.

The superior performance of Method (B) can be attributed to the following facts. In Method (A), the number of sensitivity equations is large due to the large number of variables, making the computational effort of integration expensive. In Method (B) IPOPT utilizes the exact Hessian of the Lagrangian and

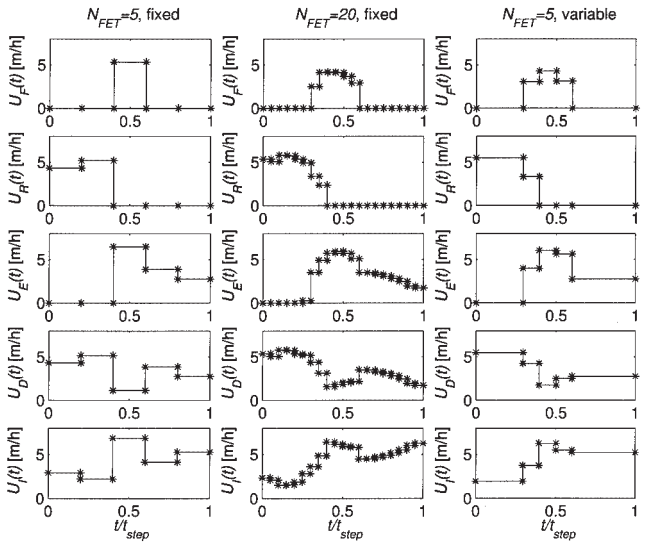

Figure 4. Optimal velocity profiles for fructose and glucose separation with N_{FET} = 5 and N_{FET} = 20.

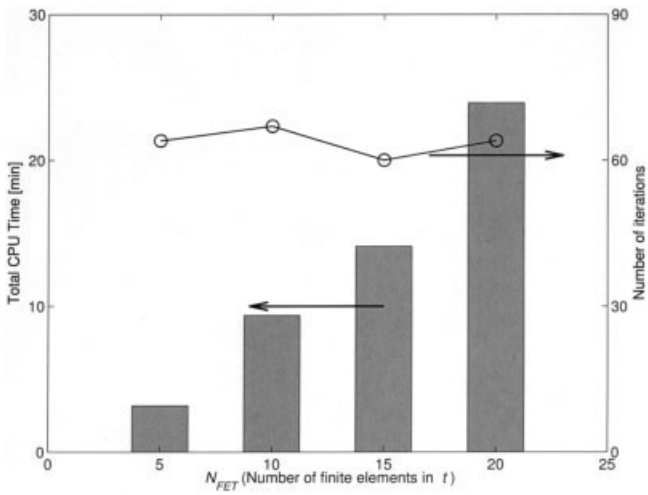

Figure 6. CPU time and number of iterations as functions of N_{FET} in PowerFeed optimization for glucose and fructose separation.

Table 4. Optimization Statistics of PowerFeed

	Fixed Finite Elements $N_{FET} = 5$	Fixed Finite Elements $N_{FET} = 20$	Variable Finite Elements $N_{FET} = 5$
CPU time [min]	3.17	23.93	6.53
Number of iterations	64	60	112
CPU time/iteration [s]	2.97	23.93	3.50
$\bar{u}_F$ (optimal value) [m/h]	1.0677	1.0752	1.0744

Comparison of fixed and variable finite elements using Method (B) for fructose and glucose separation.

sparse linear algebra. On the other hand, SRQPD in Method (A) approximates the Hessian using a quasi-Newton update formula, and deals with dense linear systems derived from sensitivity of the DAEs.

PowerFeed: variable zone velocities

With the same model parameter set, we allow the zone velocities to change dynamically in the temporal domain. In this study, we require the zone velocities to be constant in each temporal finite element. Method (B) can be easily extended to such generalizations. The same values are used for N_{FEX}, N_{FET}, and N_{COL}. The same initialization scheme is used with the same initial operating conditions as in the previous case study. First, the length of each finite elements is fixed. We do not fix $u_l(t)$ in this case study, but impose non-negative flow rate constraints

$$u_R(t),\ u_E(t),\ u_D(t) \geq 0, \qquad t\ \varepsilon\ [0,\ t_{\text{step}}] \tag{25}$$

Also for the lower bound, we set $u_l = 0$ m/h to allow the flow to stop temporarily. IPOPT finds the optimal solution in 3.17 CPU min. The optimal throughput is nearly twice as high as that of the constant flow rate problem. The optimal control profiles and optimal concentration profiles are shown in Figures 4 and 5, respectively. Again IPOPT successfully finds the optimal solution even when N_{FET} is increased (Figure 6). In spite of the increased decision variables, the number of iterations does not increase. As can be seen in Table 4, however, the optimal throughput increases only slightly even when N_{FET} is increased to 20.

In an attempt to further exploit the flexibility of PowerFeed, we allow the lengths of temporal finite elements h_l to move, within the following range

$$\frac{1}{2N_{FET}} \leq h_l \leq \frac{2}{N_{FET}}, \qquad l = 1,\ \ldots,\ N_{FET} \tag{26}$$

Table 5. Parameters for 1,1′-bi-2 Naphthol Enantiomeric Separation

Parameter	Value	Parameter	Value
ε_b	0.4	L [m]	0.105
$K_{appl\,1}$ [1/s]	0.1	$K_{appl\,2}$ [1/s]	0.1
$H_{1,1}$ [g/l]	3.73	$H_{1,2}$ [g/l]	2.69
$H_{2,1}$ [g/l]	0.30	$H_{2,2}$ [g/l]	0.10
K_{11}	0.0336	K_{12}	0.0466
K_{21}	1.0	K_{22}	3.0
$C_{F,1}$ [g/l]	3	$C_{F,2}$ [g/l]	3
N_{Column}	8	N_m	2 (all zones)

IPOPT again finds the optimal solution in 6.53 CPU min. The profiles are shown in Figure 5. As can be seen from the figures, the optimal control profiles have a similar pattern as the fixed finite elements' case. The optimal throughput has increased only slightly. The fact that the objective function does not improve despite the increased degrees of freedom is caused by the expected insensitivity to highly refined control profiles. Note that the control variables appear only linearly in the optimal control problem. This leads to a singular control problem where the response surface of the objective function has nearly zero curvature and is not sensitive to the unconstrained portions of the control profiles (singular arcs). Hence, further refinement of these profiles should not lead to noticeable improvements in the objective function.

Case Study 2: Nonlinear Isotherm

To demonstrate the reliability of Method (B), we apply our implementation to the bi-Langmuir isotherm[16]

$$q_{n,i}^{eq} = \frac{H_{1,i}C_{n,i}(x,\ t)}{1 + K_{11}C_{n,1}(x,\ t) + K_{12}C_{n,2}(x,\ t)} + \frac{H_{2,i}C_{n,i}(x,\ t)}{1 + K_{21}C_{n,1}(x,\ t) + K_{22}C_{n,2}(x,\ t)} \tag{27}$$

This isotherm takes into account the saturation of adsorption, as well as interactions between two components. In this case study, the mass-transfer resistance equation is based on the solid phase (Eq. 3). The model parameters are listed in Table 5. The operating condition given in Minceva et al.[16], listed in Table 6, is used as the initial operating point.

Constant zone velocities

After running several simulation runs, we choose $N_{FET} = 5$, $N_{FEX} = 10$, and $N_{COL} = 3$, which we confirm to be sufficiently

Table 6. Operating Conditions of 1,1′-bi-2 Naphthol Enantiomeric Separation

Variable	Initial Value	Optimal Value
$\bar{u}_I$ (fixed) [m/h]	6.424	6.424
$\bar{u}_{II}$ [m/h]	4.391	4.316
$\bar{u}_{III}$ [m/h]	4.803	5.222
$\bar{u}_{IV}$ [m/h]	3.999	3.596
t_{step} [s]	180	173.7
$\bar{u}_F = \bar{u}_{III} - \bar{u}_{II}$ [m/h]	0.412	0.9058
Extract purity [%]	93.66	97.00
Extract recovery [%]	98.05	80.00

Initial values and optimal values of constant flow rate operation using Method (B). Total CPU time for this optimization is 1.76 minutes.

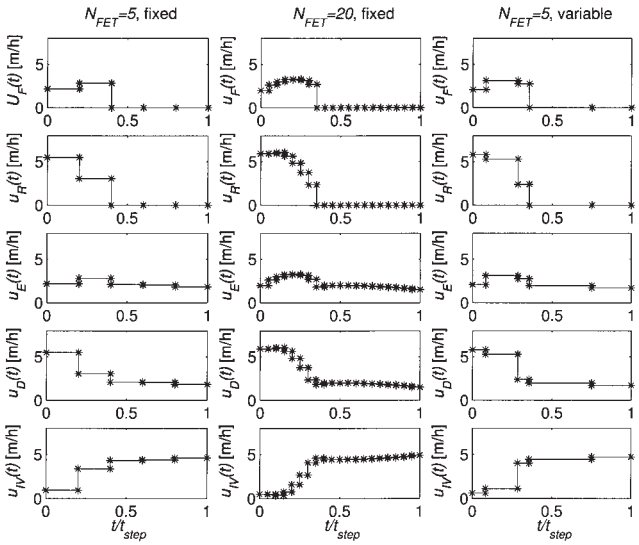

Figure 7. Optimal control profiles of 1,1′-bi-2 naphthol enantiomeric separation.

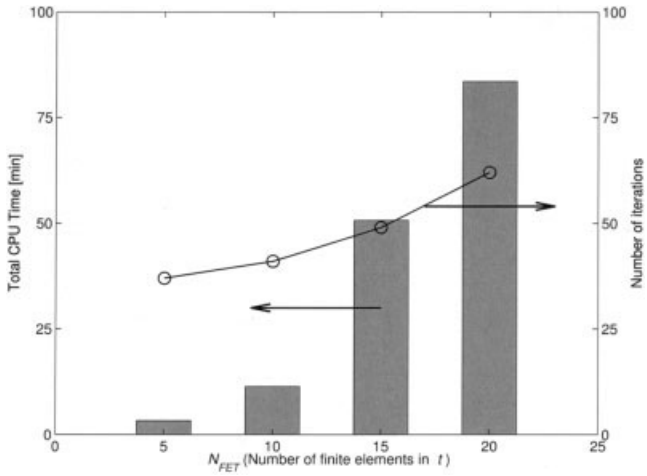

Figure 8. CPU time and number of iterations as functions of N_{FET} in PowerFeed optimization for 1,1′-bi-2 naphthol enantiomeric separation.

accurate. We keep the same recovery requirement, $Rec_{\min} = 80\%$, but choose a higher purity requirement, $Pur_{min} = 97\%$. The bounds on the zone velocities are $u_l = 0.1$ m/h and $u_u = 6.424$ m/h. The same initialization scheme as the case study of fructose/glucose separation is used, although the purity requirement is not satisfied at the initial point. The initialization took 61 CPU s using IPOPT in AMPL. Then the initial concentration profiles and initial operating conditions are given to the optimization problem. The number of variables is 18071, and number of equations is 18067. IPOPT finds the optimal solution in 1.76 min with 17 iterations. The optimal solution is listed in Table 6. Since the initial operating condition is relatively close to the optimal one, the number of iterations is small. We can confirm that even if N_{FET} is increased from 5 to 20, the variation of optimal throughput is less than 0.1%, and any change of the concentration profiles can not be seen. We conclude that $N_{FET} = 5$ and $N_{COL} = 3$ are sufficient also for this case study.

PowerFeed: variable zone velocities

We also consider the optimization of PowerFeed operation with the parameter set in Table 5. The parameters and initialization scheme are the same as those in the previous case study. With the fixed length of finite elements, IPOPT finds the optimal solution in 3.27 min. The optimal control profiles and concentration profiles are shown in Figures 7 and 9, respectively. The optimal throughput increases by about 10% due to the saturation effect of the adsorbent. IPOPT successfully converged even when the number of finite elements in time is increased to 20 (Table 7). As can be seen in the table, the optimal throughput does not increase despite the increased number of the operating parameters. The CPU time and number of iterations are plotted as a function of N_{FET} in Figure 8. The increase of the number of iterations is moderate as N_{FET} increases. Again, we attempt to improve the throughput further by allowing the finite element lengths to move. Using the same bounds from Eq. 26, IPOPT finds the optimal solution in 6.73 CPU min. The optimal concentration profiles are shown also in Figure 9.

Conclusion and Future Work

Single and full discretization methods are implemented for optimization problems for SMB processes. In the first case study with a linear isotherm, the full-discretized method using AMPL and IPOPT has been found to be superior to the single-discretized method using gPROMS with SRQPD. Also the simultaneous method has been shown to be easily extended to PowerFeed operation with both linear and bi-Langmuir isotherms. Despite the large number of variables, IPOPT shows good convergence properties in both case studies. It has been shown that our method can be easily applied to PowerFeed systems. In both cases of linear and bi-Langmuir isotherms, the optimal throughput has been increased from constant flow rate operation. However, in the case study of PowerFeed systems, the optimal throughput does not increase further when the number of temporal finite elements is increased, due to control profile insensitivity in this singular control problem. Our future

Table 7. Optimization Statistics of PowerFeed

	Fixed Finite Elements: $N_{FET} = 5$	Fixed Finite Elements: $N_{FET} = 20$	Variable Finite Elements $N_{FET} = 5$
CPU time [min]	3.26	83.56	6.73
Number of iterations	37	62	82
CPU time per iteration [s]	5.297	80.87	4.926
Optimal value [m/h]	0.9925	0.9947	0.9944

Comparison of fixed and variable finite elements using Method (B) for 1,1′-bi-2 naphthol enantiomeric separation.

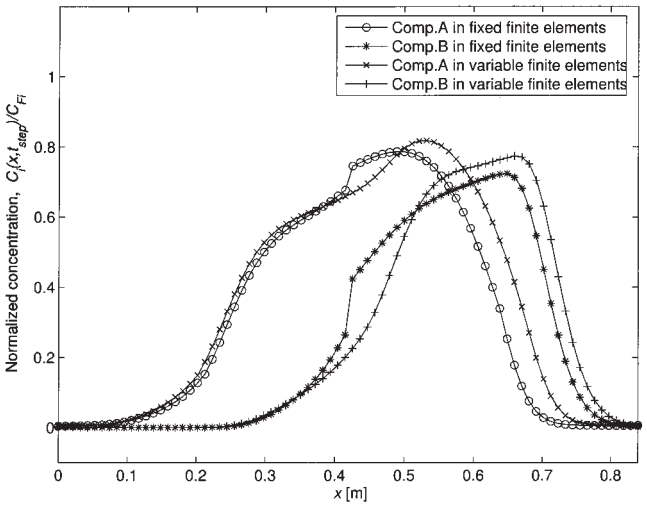

Figure 9. Optimal concentration profiles of 1,1′-bi-2 naphthol enantiomeric separation: Fixed finite elements of time and variable finite elements.

work will consider optimal column configuration, which can be formulated as a mixed integer nonlinear programming (MINLP), and online optimization schemes. In these future studies, where availability of a fast NLP solver is crucial, our simultaneous method can be a promising candidate.

Acknowledgments

The authors gratefully acknowledge the support of Dr. Daeho Ko in gPROMS implementation. Funding from the National Science Foundation under Grant CTS-0314647 is gratefully acknowledged.

Literature Cited

1. Subramani HJ, Hidajat K, Ray AK. Optimization of reactive SMB and Varicol systems. *Comp and Chem Eng*. 2003;27:1883-1901.
2. Dünnebier G, Klatt K-U. Modelling and simulation of nonlinear chromatographic separation processes: a comparison of different modeling approaches. *Chem Eng Sci*. 2000;55:373-380.
3. Kloppenburg E, Gilles ED. A new concept for operating simulated moving-bed processes'. *Chem Eng & Technol*. 1999;22(10):813-817.
4. Toumi A. *Optimaler Betrieb und Regelung von Simulated-Moving-Bed-Prozessen*. PhD thesis, Universität Dortmund: Shaker Verlag; Aachen, Germany; 2005.
5. Toumi A, Hanisch F, Engell S. Optimal operation of continuous chromatographic processes: Mathematical optimization of the VARICOL process. *Indust and Eng Chem Res*. 2002;41:4328-4337.
6. van Deemter JJ, Zuiderweg FJ, Klinkenberg A. Longitudinal diffusion and resistance to mass transfer as causes of nonideality in chromatography. *Chem Eng Sci*. 1956;5:271-289.
7. Golshan-Shirazi S, Guiochon G. Comparison of the various kinetic models of non-linear chromatography. *J of Chromatography*. 2003; 603:1-11.
8. Ching CB, Lu ZP. Parabolic intraparticle concentration profile assumption in modelling and simulation of nonlinear simulated moving-bed separation processes. *Chem Eng Sci*. 1998;53(6):1311-1315.
9. Hashimoto K, Adachi S, Noujima H, Maruyama H. Models for the separation of glucose/fructose mixture using a simulated moving bed adsorber. *J of Chem Eng of Japan*. 1983;16(5):400-406.
10. Jiang L, Biegler LT, Grant Fox V. Simulation and optimization of pressure swing adsorption systems for air separation. *AIChE J*. 2003; 49(5):1140-1157.
11. Nilchan S. *The optimisation of periodic adsorption processes*. University of London, London, U.K; 1997. PhD thesis.
12. Ko D, Siriwardane R, Biegler LT. Optimization of a pressure-swing adsorption process using zeolite 13X for CO2 sequestration. *Ind and Eng Chem Res*. 2003;42:339-348.
13. Kameswaran S, Biegler LT, Staus GH. Dynamic optimization for the coreflooding problem in reservoir engineering. *Computers and Chemical Engineering*. 2005;29:1787–1800.
14. Biegler LT, Cervantes AM, Wächter A. Advances in simultaneous strategies for dynamic process optimization. *Chem Eng Sci*. 2002;57: 575-593.
15. Wächter A, Biegler LT. On the implementation of an interior-point filter linesearch algorithm for large-scale nonlinear programming. Research Report RC 23149, IBM T. J. Watson Research Center, Yorktown; 2004.
16. Minceva M, Pais LS, Rodrigues AE. Cyclic steady state of simulated moving bed processes for enantiomer separation. *Chem Eng and Proc*. 2003;42:93-104.

Manuscript received May 19, 2005, and revision received Sept. 25, 2005.